Journal of Sound and Vibration (1999) **220**(5), 827–846
Article No. jsvi.1998.1970, available online at http://www.idealibrary.com.on IDEAL

VIBRATION CONTROL SIMULATION OF LAMINATED COMPOSITE PLATES WITH INTEGRATED PIEZOELECTRICS

G. R. Liu, X. Q. Peng and K. Y. Lam

Department of Mechanical and Production Engineering, *National University of Singapore*, 10 *Kent Ridge Crescent*, *Singapore* 119260

AND

J. Tani

Institute of Fluid Science, *Tohoku University*, *Sendai* 980, *Japan*

(*Received* 12 *September* 1997, *and in final form* 2 *September* 1998)

A finite element formulation is presented to model the dynamic as well as static response of laminated composite plates containing integrated piezoelectric sensors and actuators subjected to both mechanical and electrical loadings. The formulation is based on the classical laminated plate theory and Hamilton's principle. In this formulation, the mass and stiffness of the piezo-layers have been taken into account. A four-node non-conforming rectangular plate bending element is implemented for the analysis. A simple negative velocity feedback control algorithm coupling the direct and converse piezoelectric effects is used to actively control the dynamic response of an integrated structure through a closed control loop. The model is validated by comparison with existing results documented in the literature. Several numerical examples are presented. The influence of stacking sequence and position of sensors/actuators on the response of the plate is evaluated.

1. INTRODUCTION

The rapid development of space structures and high-performance flexible mechanical system has stimulated extensive research into smart structures and systems over the past several years. A smart structure can be defined as a structure or structural component with bonded or embedded sensors and actuators as well as control systems, which change the shape and dynamic behavior of the structure. Smart structures and systems have self-inspection and inherent adaptive capabilities. They can respond almost instantaneously to the changes in the external environment and hence can greatly enhance the performance of existing structures. The research and implementation of smart structures and systems opens new opportunities for radical changes in the design of adaptive structures and high-performance structures.

0022–460X/99/100827 + 20 $30.00/0

Recent studies on smart structures have shown that piezoelectric materials can be an effective alternative to the conventional discrete sensing and control systems. Piezoelectric materials have coupled mechanical and electrical properties. They generate an electric charge when subjected to a mechanical deformation, a property called the *direct piezoelectic effect*. Conversely, mechanical stress or strain is produced by an applied electric field, which is called the *converse piezoelectric effect*. Bonding or embedding piezoelectric patches in a structure can act as sensors to monitor or as actuators to control the response of the structure. In addition, piezoelectric materials have several other attractive advantages such as fast response, large force output, being inexpensive and lightweight.

Additionally, advances in design and manufacturing technologies have greatly enhanced the use of advanced composite materials for aircraft and aerospace structural applications. Due to their structural advantages of high stiffness-to-weight strength-to-weight ratios, composite materials can be used in the design of smart structures and hence significantly improve the performance of aircraft and space structures. Investigators have developed several analytical and numerical models for the laminated composite structures with integrated piezoelectric sensors and actuators. The simplest and often used model is the equivalent single layer model, which includes the classical laminated plate theory [1–3], first order shear deformation theory [4–7] and higher-order theory [8]. Another model for thick laminated composite structures is layerwise theory [9–11]. Besides, some 3-D models [12–16] and hybrid model [17] are also available. These models have their own advantages and disadvantages in terms of the accuracy, efficiency and computational effort.

In this paper, a finite element model is developed for the shape control and active vibration suppression of laminated composite plates with integrated piezoelectric sensors and actuators. The model is based on the classical laminated plate theory and the principle of virtual displacements. Four-node rectangular non-conforming plate bending elements are used to model the laminated composite plate. The direct piezoelectric equation is used to calculate the total charge created by the strains on the sensor electrodes; and the actuators provide a damping effect on the composite plate by coupling a negative velocity feedback control algorithm in a closed control loop. A Fortran program has been made using the derived formulation. The model is validated by comparing with results available in the literature. It is then used to simulate the shape control and active free vibration suppression of a simply supported laminated composite plate. The effect of stacking sequence and position of sensors/actuators on the response of the plate is also investigated.

2. PIEZOELECTRIC EQUATIONS

A laminated composite plate with integrated sensors and actuators is shown in Figure 1. It is assumed that each layer of the plate possesses a plane of elastic

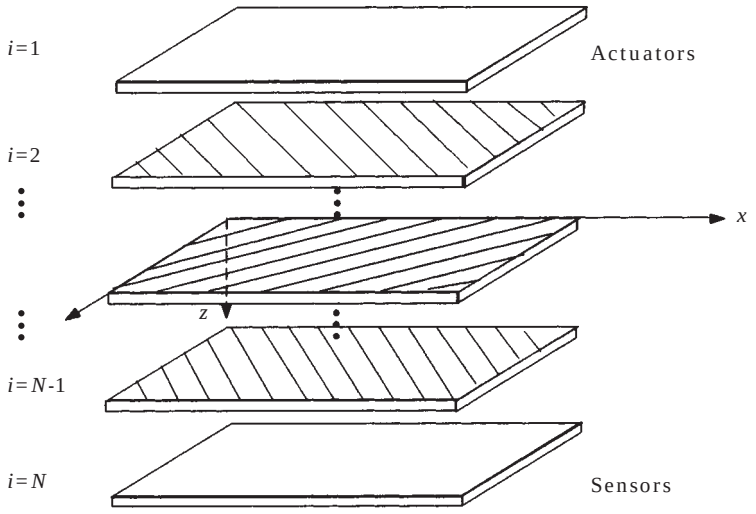

Figure 1. A typical laminated piezoelectric composite plate.

symmetry parallel to the x–y plane, the kth layer's lamina constitutive equations coupling the direct and converse piezoelectric equations can be expressed as [18]:

$$\begin{Bmatrix} D_1 \\ D_2 \\ D_3 \end{Bmatrix}_k = \begin{bmatrix} 0 & 0 & 0 \\ 0 & 0 & 0 \\ \bar{e}_{31} & \bar{e}_{32} & 0 \end{bmatrix}_k \begin{Bmatrix} \varepsilon_1 \\ \varepsilon_2 \\ \varepsilon_6 \end{Bmatrix}_k + \begin{bmatrix} \bar{\epsilon}_{11} & 0 & 0 \\ 0 & \bar{\epsilon}_{22} & 0 \\ 0 & 0 & \bar{\epsilon}_{33} \end{bmatrix}_k \begin{Bmatrix} E_1 \\ E_2 \\ E_3 \end{Bmatrix}_k \tag{1}$$

$$\begin{Bmatrix} \sigma_1 \\ \sigma_2 \\ \sigma_6 \end{Bmatrix}_k = \begin{bmatrix} \bar{Q}_{11} & \bar{Q}_{12} & 0 \\ \bar{Q}_{12} & \bar{Q}_{22} & 0 \\ 0 & 0 & \bar{Q}_{66} \end{bmatrix}_k \begin{Bmatrix} \varepsilon_1 \\ \varepsilon_2 \\ \varepsilon_6 \end{Bmatrix}_k - \begin{bmatrix} 0 & 0 & \bar{e}_{31} \\ 0 & 0 & \bar{e}_{32} \\ 0 & 0 & 0 \end{bmatrix}_k \begin{Bmatrix} E_1 \\ E_2 \\ E_3 \end{Bmatrix}_k \tag{2}$$

where $(\bar{Q}_{ij}, \bar{e}_{ij}, \bar{\epsilon}_{ij})$ are, respectively, the plane-stress reduced elastic constants, the piezoelectric constants and the permittivity coefficients of the kth lamina in its material coordinate system, and $(\sigma_i, \varepsilon_i, E_i, D_i)$ are the stress, strain, electric field and electric displacement components, respectively, to the material coordinate system. The plane-stress reduced elastic constants $\bar{Q}_{ij}$ are given as

$$\bar{Q}_{11} = \frac{E_1}{1 - \nu_{12}\nu_{21}}, \qquad \bar{Q}_{12} = \frac{\nu_{12}E_2}{1 - \nu_{12}\nu_{21}} \tag{3}$$

$$\bar{Q}_{22} = \frac{E_2}{1 - \nu_{12}\nu_{21}}, \qquad \bar{Q}_{66} = G_{12}. \tag{4}$$

It should be noted that the piezoelectric constant matrix $[\bar{e}]$ in equation (1) is sometimes unavailable and it can be expressed in terms of the commonly available piezoelectric strain constant matrix $[d]$ using the relation

$$[\bar{e}] = [d][\bar{Q}] \tag{5}$$

where

$$[d] = \begin{bmatrix} 0 & 0 & 0 \\ 0 & 0 & 0 \\ d_{31} & d_{32} & 0 \end{bmatrix}. \tag{6}$$

Upon transformation, the lamina piezoelectric equations can be expressed in terms of the stresses, strains and electric displacements in the plate coordinates as

$$\begin{Bmatrix} D_x \\ D_y \\ D_z \end{Bmatrix}_k = \begin{bmatrix} 0 & 0 & 0 \\ 0 & 0 & 0 \\ e_{31} & e_{32} & e_{36} \end{bmatrix}_k \begin{Bmatrix} \varepsilon_x \\ \varepsilon_y \\ \gamma_{xy} \end{Bmatrix}_k + \begin{bmatrix} \epsilon_{11} & \epsilon_{12} & 0 \\ \epsilon_{12} & \epsilon_{22} & 0 \\ 0 & 0 & \epsilon_{33} \end{bmatrix}_k \begin{Bmatrix} E_x \\ E_y \\ E_z \end{Bmatrix}_k \tag{7}$$

$$\begin{Bmatrix} \sigma_x \\ \sigma_y \\ \sigma_{xy} \end{Bmatrix}_k = \begin{bmatrix} Q_{11} & Q_{12} & Q_{16} \\ Q_{12} & Q_{22} & Q_{26} \\ Q_{16} & Q_{26} & Q_{66} \end{bmatrix}_k \begin{Bmatrix} \varepsilon_x \\ \varepsilon_y \\ \gamma_{xy} \end{Bmatrix}_k - \begin{bmatrix} 0 & 0 & e_{31} \\ 0 & 0 & e_{32} \\ 0 & 0 & e_{36} \end{bmatrix}_k \begin{Bmatrix} E_x \\ E_y \\ E_z \end{Bmatrix}_k. \tag{8}$$

Equations (7) and (8) can also be written as

$$\{D\}_k = [e]_k \{\varepsilon\}_k + [\epsilon]_k \{E\}_k \tag{9}$$

$$\{\sigma\}_k = [Q]_k \{\varepsilon\}_k - [e]_k^{\mathrm{T}} \{E\}_k. \tag{10}$$

3. CLASSICAL LAMINATED PLATE THEORY

The classical laminated plate theory (CLPT) is based on the Kirchhoff assumption, which leads to the displacement field [18]

$$u(x, y, z, t) = u_0(x, y, t) - z \frac{\partial w_0}{\partial x} \tag{11}$$

$$v(x, y, z, t) = v_0(x, y, t) - z \frac{\partial w_0}{\partial y} \tag{12}$$

$$w(x, y, z, t) = w_0(x, y, t) \tag{13}$$

where u, v and w are the displacement components in the x-, y- and z-directions, respectively, and (u_0, v_0, w_0) are the midplane displacements.

We define

$$\{u\} = \{u \quad v \quad w\}^{\mathrm{T}}$$

$$\{\bar{u}\} = \{u_0 \quad v_0 \quad w_0 \quad \partial w_0/\partial x \quad \partial w_0/\partial y\}^{\mathrm{T}}$$

where $\{\bar{u}\}$ is the nodal degrees-of-freedom. Then equations (11)–(13) can be rewritten as

$$\{u\} = [H]\{\bar{u}\} \tag{14}$$

where

$$[H] = \begin{bmatrix} 1 & 0 & 0 & -z & 0 \\ 0 & 1 & 0 & 0 & -z \\ 0 & 0 & 1 & 0 & 0 \end{bmatrix}. \tag{15}$$

In this work, the rectangular non-conforming plate bending element [18] is used. The generalized displacements u_0 and v_0 are interpolated over an element as

$$u_0(x, y, t) = \sum_{i=1}^{4} u_{0i}(t)\psi_i(x, y) \tag{16}$$

$$v_0(x, y, t) = \sum_{i=1}^{4} v_{01}(t)\psi_i(x, y) \tag{17}$$

where ψ_i are the linear interpolation functions

$$\psi_i = \tfrac{1}{4}(1 + \xi\xi_i)(1 + \eta\eta_i) \qquad i = 1, 2, 3, 4 \tag{18}$$

w_0 is interpolated over an element as

$$w_0(x, y, t) = \sum_{i=1}^{4} \left[w_{0i}(t)g_{i1}(x, y) + \frac{\partial w_{0i}(t)}{\partial x} g_{i2}(x, y) + \frac{\partial w_{0i}(t)}{\partial y} g_{i3}(x, y) \right] \tag{19}$$

where g_{ij} $(j = 1, 2, 3)$ are the non-conforming Hermite cubic interpolation functions

$$g_{i1} = \tfrac{1}{8}(1 + \xi\xi_i)(1 + \eta\eta_i)(2 + \xi\xi_i + \eta\eta_i - \xi^2 - \eta^2) \tag{20}$$

$$g_{i2} = \tfrac{1}{8}\xi_i(1 + \xi\xi_i)^2(\xi\xi_i - 1)(1 + \eta\eta_i)a_0 \tag{21}$$

$$g_{i3} = \tfrac{1}{8}\eta_i(1 + \eta\eta_i)^2(\eta\eta_i - 1)(1 + \xi\xi_i)b_0 \qquad i = 1, 2, 3, 4 \tag{22}$$

where a_0 and b_0 are the half length of the rectangular element along x- and y-directions respectively.

Substituting equations (16), (17) and (19) into equation (14) yields

$$\{u\} = [H][N]\{u^e\} \tag{23}$$

where

$$[N] = [[N_1] \quad [N_2] \quad [N_3] \quad [N_4]] \tag{24}$$

$$[N_i] = \begin{bmatrix} \psi_i & 0 & 0 & 0 & 0 \\ 0 & \psi_i & 0 & 0 & 0 \\ 0 & 0 & g_{i1} & g_{i2} & g_{i3} \\ 0 & 0 & \dfrac{\partial g_{i1}}{\partial x} & \dfrac{\partial g_{i2}}{\partial x} & \dfrac{\partial g_{i3}}{\partial x} \\ 0 & 0 & \dfrac{\partial g_{i1}}{\partial y} & \dfrac{\partial g_{i2}}{\partial y} & \dfrac{\partial g_{i3}}{\partial y} \end{bmatrix} \qquad i = 1, 2, 3, 4. \tag{25}$$

The non-zero infinitesimal strains associated with the displacements are given by

$$\begin{Bmatrix} \varepsilon_x \\ \varepsilon_y \\ \gamma_{xy} \end{Bmatrix} = \begin{Bmatrix} \dfrac{\partial u}{\partial x} \\ \dfrac{\partial v}{\partial y} \\ \dfrac{\partial u}{\partial y} + \dfrac{\partial v}{\partial x} \end{Bmatrix} = \begin{Bmatrix} \dfrac{\partial u_0}{\partial x} \\ \dfrac{\partial v_0}{\partial y} \\ \dfrac{\partial u_0}{\partial y} + \dfrac{\partial v_0}{\partial x} \end{Bmatrix} - z \begin{Bmatrix} \dfrac{\partial^2 w_0}{\partial x} \\ \dfrac{\partial^2 w_0}{\partial y^2} \\ 2\dfrac{\partial^2 w_0}{\partial x\, \partial y} \end{Bmatrix} \tag{26}$$

or, in vector form

$$\{\varepsilon\} = \{\varepsilon^{(0)}\} - z\{\varepsilon^{(1)}\}. \tag{27}$$

Substituting equation (23) into equation (26) yields

$$\{\varepsilon\} = [B]\{u^e\} \tag{28}$$

where

$$[B] = [[B_1] \quad [B_2] \quad [B_3] \quad [B_4]] = [A] - z[C] \tag{29}$$

$$[B_i] = [A_i] - z[C_i] \tag{30}$$

$$[A_i] = \begin{bmatrix} \dfrac{\partial \psi_i}{\partial x} & 0 & 0 & 0 & 0 \\ 0 & \dfrac{\partial \psi_i}{\partial y} & 0 & 0 & 0 \\ \dfrac{\partial \psi_i}{\partial y} & \dfrac{\partial \psi_i}{\delta x} & 0 & 0 & 0 \end{bmatrix} \tag{31}$$

$$[C_i] = \begin{bmatrix} 0 & 0 & \dfrac{\partial^2 g_{i1}}{\partial x^2} & \dfrac{\partial^2 g_{i2}}{\partial x^2} & \dfrac{\partial^2 g_{i3}}{\partial x^2} \\ 0 & 0 & \dfrac{\partial^2 g_{i1}}{\partial y^2} & \dfrac{\partial^2 g_{i2}}{\partial y^2} & \dfrac{\partial^2 g_{i3}}{\partial y^2} \\ 0 & 0 & 2\dfrac{\partial^2 g_{i1}}{\partial x\, \partial y} & 2\dfrac{\partial^2 g_{i2}}{\partial x\, \partial y} & 2\dfrac{\partial^2 g_{i3}}{\partial x\, \partial y} \end{bmatrix} \qquad i = 1, 2, 3, 4. \tag{32}$$

4. FINITE ELEMENT MODEL

4.1. DYNAMIC EQUATIONS

To derive dynamic equations of motion for the laminated composite plate with integrated piezoelectric sensors and actuators, we use Hamilton's principle:

$$\delta \int_{t_1}^{t_2} [T - U + W] \, \mathrm{d}t = 0 \tag{33}$$

where T is the kinetic energy, U is the strain energy, and W is the work done by the applied forces. To account for the sensors' mass and actuator's mass and stiffness, the piezoelectric layers are treated as other layers with different material properties in deriving the dynamic equations of motion.

The kinetic energy at the element level is defined as

$$T^e = \frac{1}{2} \int_{V_e} \rho \{\dot{u}\}^{\mathrm{T}} \{\dot{u}\} \, \mathrm{d}v \tag{34}$$

where V_e is the volume of the plate element. The strain energy can be written as

$$U^e = \frac{1}{2} \int_{V_e} \{\varepsilon\}^{\mathrm{T}} \{\sigma\} \, \mathrm{d}v. \tag{35}$$

The work done by the external forces is

$$W^e = \int_{V_e} \{u\}^{\mathrm{T}} \{f_b\} \, \mathrm{d}v + \int_{S_1} \{u\}^{\mathrm{T}} \{f_s\} \, \mathrm{d}s + \{u\}^{\mathrm{T}} \{f_c\} \tag{36}$$

where $\{f_b\}$ is the body force, S_1 is the surface area of the plate element where the surface force $\{f_s\}$ is specified and $\{f_c\}$ is the concentrated load.

We assume that the quasi-static electric field vector $\{E\}$ can be defined by the electrical potential ϕ as

$$E = -\nabla \phi \tag{37}$$

where ∇ denotes the gradient operator.

When a voltage V^e is applied to the actuator layer with thickness h_A in the thickness direction, the electric field vector $\{E\}$ can be expressed as

$$\{E\} = \{0 \quad 0 \quad 1/h_A\}^{\mathrm{T}} V^e = \{B_v\} V^e. \tag{38}$$

Substituting equations (34)–(36) into equation (33) and using equations (10), (23), (28) and (38), the dynamic matrix equations can be written as

$$[M^e]\{\ddot{u}^e\} + [K^e]\{u^e\} = \{F^e\} + \{K^e_{av}\} V^e \tag{39}$$

where

$$\{K_{av}^e\} = \int_{V_e} [B]^{\mathrm{T}}[e]^{\mathrm{T}}\{B_v\}\,\mathrm{d}v = \{K_1^e\} - \{K_2^e\} \tag{40}$$

$$[M^e] = \sum_{k=1}^{N_L} \int_{-1}^{1}\int_{-1}^{1} \rho_k [N]^{\mathrm{T}}\left[\int_{z_k}^{z_{k+1}} [H]^{\mathrm{T}}[H]\,\mathrm{d}z\right][N]|J|\,\mathrm{d}\xi\,\mathrm{d}\eta \tag{41}$$

$$[K^e] = \int_{V_e} [B]^{\mathrm{T}}[Q][B]\,\mathrm{d}v = [K_A^e] - [K_{AC}^e] - [K_{AC}^e]^{\mathrm{T}} + [K_C^e] \tag{42}$$

$$\{F^e\} = \int_{V_e} [N]^{\mathrm{T}}[H]^{\mathrm{T}}\{f_b\}\,\mathrm{d}v + \int_{S_1} [N]^{\mathrm{T}}[H]^{\mathrm{T}}\{f_s\}\,\mathrm{d}s + [N]^{\mathrm{T}}[H]^{\mathrm{T}}\{f_c\} \tag{43}$$

where

$$\{K_1^e\} = \sum_{k=1}^{N_L} (z_{k+1} - z_k) \int_{-1}^{1}\int_{-1}^{1} [A]^{\mathrm{T}}[e]_k^{\mathrm{T}}\{B_v\}|J|\,\mathrm{d}\xi\,\mathrm{d}\eta \tag{44}$$

$$\{K_2^e\} = \sum_{k=1}^{N_L} \frac{1}{2}(z_{k+1}^2 - z_k^2) \int_{-1}^{1}\int_{-1}^{1} [C]^{\mathrm{T}}[e]_k^{\mathrm{T}}\{B_v\}|J|\,\mathrm{d}\xi\,\mathrm{d}\eta \tag{45}$$

$$[K_A^e] = \sum_{k=1}^{N_L} (z_{k+1} - z_k) \int_{-1}^{1}\int_{-1}^{1} [A]^{\mathrm{T}}[Q]_k[A]|J|\,\mathrm{d}\xi\,\mathrm{d}\eta \tag{46}$$

$$[K_{AC}^e] = \sum_{k=1}^{N_L} \frac{1}{2}(z_{k+1}^2 - z_k^2) \int_{-1}^{1}\int_{-1}^{1} [A]^{\mathrm{T}}[Q]_k[C]|J|\,\mathrm{d}\xi\,\mathrm{d}\eta \tag{47}$$

$$[K_C^e] = \sum_{k=1}^{N_L} \frac{1}{3}(z_{k+1}^3 - z_k^3) \int_{-1}^{1}\int_{-1}^{1} [C]^{\mathrm{T}}[Q]_k[C]|J|\,\mathrm{d}\xi\,\mathrm{d}\eta \tag{48}$$

and N_L denotes the number of layers and J is the Jacobian matrix.

Assembling the element equations gives the global dynamic equation

$$[\mathbf{M}]\{\ddot{\mathbf{u}}\} + [\mathbf{C}]\{\dot{\mathbf{u}}\} + [\mathbf{K}]\{\mathbf{u}\} = \{\mathbf{F}\} + \{\mathbf{F}_{\mathrm{v}}\} \tag{49}$$

where $\{\mathbf{F}\}$ is the external mechanical force vector and $\{\mathbf{F}_{\mathrm{v}}\}$ is the electrical force vector:

$$\{\mathbf{F}_{\mathrm{v}}\} = \{\mathbf{K}_{\mathbf{av}}\}\{\mathbf{V}\}. \tag{50}$$

4.2. SENSOR EQUATION

Since no external electric field is applied to the sensor layer and the charge is collected only in the thickness direction, only the electric displacement D_z is of interest, and it can be derived from equation (7) as

$$D_z = e_{31}\varepsilon_x + e_{32}\varepsilon_y + e_{36}\gamma_{xy} = \{e_3\}\{\varepsilon\} \tag{51}$$

where

$$\{e_3\} = \{e_{31} \quad e_{32} \quad e_{36}\}. \tag{52}$$

The total charge developed on the sensor surface is the spatial summation of all the point charges on the sensor layer. Hence, the closed circuit charge measured through the electrodes of a sensor patch in the kth layer is [19]

$$q(t) = \frac{1}{2}\left[\int_{S_{2(z=z_k)}} D_z \, \mathrm{d}S + \int_{S_{2(z=z_{k+1})}} D_z \, \mathrm{d}S\right] \tag{53}$$

where S_2 is the effective surface electrode of the patch, which defines the integration domain where all the points are covered with surface electrode on both sides of the sensor lamina. In the present work, it is assumed that the whole piezoelectric lamina serves as the effective surface electrode.

Assuming that the sensor patch covers several elements, then the total charge $q(t)$ can be written as follows:

$$q(t) = \sum_{j=1}^{N_s} \frac{1}{2}\left[\int_{S_{j(z=z_k)}} D_z \, \mathrm{d}S + \int_{S_{j(z=z_{k+1})}} D_z \, \mathrm{d}S\right] \tag{54}$$

where N_s denotes the number of elements and S_j is the surface of the jth element.

Using equations (28) and (51), equation (54) can be rewritten as

$$q(t) = \sum_{j=1}^{N_s}\left[\frac{1}{2}\int_{-1}^{1}\int_{-1}^{1} \{e_3\}(-(z_k + z_{k+1})[B])|J| \, \mathrm{d}\xi \, \mathrm{d}\eta\right]\{u_j^e\}. \tag{55}$$

The current on the surface of a sensor can be expressed as

$$i(t) = \frac{\mathrm{d}q(t)}{\mathrm{d}t}. \tag{56}$$

When the piezoelectric sensors are used as strain rate sensors, the current can be converted into the open circuit sensor voltage output V_S as

$$V_S(t) = G_c i(t) = G_c \frac{\mathrm{d}q(t)}{\mathrm{d}t} \tag{57}$$

where G_c is the gain of the current amplifier.

4.3. ACTIVE CONTROL OF DAMPING

The distributed sensor generates a voltage when the structure is oscillating; and this signal is fed back into the distributed actuator using a control algorithm, as

shown in Figure 4. The actuating voltage V^e under a constant gain control algorithm can be expressed as

$$V^e = G_i V_S = G_i G_c \frac{\mathrm{d}q}{\mathrm{d}t} \tag{58}$$

where G_i is the gain to provide feedback control. It must be noted that the higher order modes may become unstable with the increase of control gain. In this paper, we mainly consider the lower order modes which are predominant in vibration suppression problems.

Substituting equation (55) into equation (58) yields

$$V^e = G \sum_{j=1}^{N_s} \{K_{sv}^j\}\{\dot{u}_j^e\} \tag{59}$$

where

$$\{K_{sv}^j\} = \frac{1}{2}\int_{-1}^{1}\int_{-1}^{1} \{e_3\}(-(z_k + z_{k+1})[B])|J| \,\mathrm{d}\xi \,\mathrm{d}\xi \tag{60}$$

$$G = G_i G_c. \tag{61}$$

Hence the system actuating voltages can be written as

$$\{\mathbf{V}\} = [\mathbf{G}]\{\mathbf{K_{sv}}\}\{\dot{\mathbf{u}}\} \tag{62}$$

where [**G**] is the control gain matrix, which provides an uncoupled collocated control.

In the feedback control, the electrical force vector $\{\mathbf{F}_v\}$ can be regarded as a feedback force. Substituting equation (62) into equation (50) gives

$$\{\mathbf{F}_v\} = \{\mathbf{K_{av}}\}[\mathbf{G}]\{\mathbf{K_{sv}}\}\{\dot{\mathbf{u}}\}. \tag{63}$$

We define

$$[\mathbf{C}^*] = -\{\mathbf{K_{av}}\}[\mathbf{G}]\{\mathbf{K_{sv}}\}. \tag{64}$$

Thus, the system equation of motion equation (49) becomes

$$[\mathbf{M}]\{\ddot{\mathbf{u}}\} + ([\mathbf{C}] + [\mathbf{C}^*])\{\dot{\mathbf{u}}\} + [\mathbf{K}]\{\mathbf{u}\} = \{\mathbf{F}\}. \tag{65}$$

As shown in equation (65), the voltage control algorithm equation (58) has a damping effect on the vibration suppression of a distributed system.

It must be noted that the damping matrix in equation (65) is not diagonal but diagonally dominant. This cannot guarantee the stability of the control system. Hence, the stability of a given control system must be examined so that an appropriate control gain can be chosen.

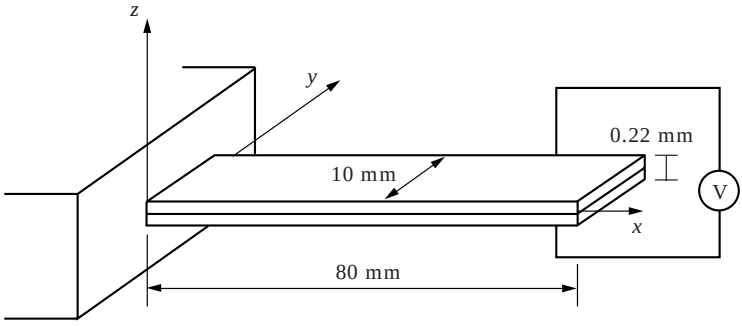

Figure 2. Piezoelectric KYNAR cantilever beam.

5. NUMERICAL EXAMPLES AND DISCUSSION

Two cases are studied in this section. The first case is the static analysis of a cantilever beam. The results obtained are compared with Koconis *et al*. [4] to validate the proposed model. The second case involves the shape control and active free vibration suppression of a simply supported laminated composite plate by integrated piezoelectric sensors and actuators. The influence of feedback control gain, ply orientation and the sensor/actuators' position on the response of the plate is analyzed.

5.1. PIEZOELECTRIC CANTILEVER BEAM

The cantilever beam, which consists of two identical layers of KYNAR piezofilm, is shown in Figure 2. The material properties for KYNAR are listed in Table 1. The beam is evenly discretized into eight plate elements.

Various external voltages between 0 and 500 V are applied to the KYNAR piezofilms. The applied external voltages induce strain in the beam, which generates forces to bend the cantilever. The calculated tip deflections of the cantilever beam are shown in Figure 3. It is seen that the results obtained by the present model are in good agreement with those of Koconis *et al*. [4].

TABLE 1

Material properties

	KYNAR	G-1195	T300/976
E_1 (GPa)	6·85	63·0	150·0
E_2 (GPa)	6·85	63·0	9·0
ν_{12}	0·29	0·29	0·3
G_{12} (GPa)	0·078	24·8	7·1
G_{13} (GPa)	–	–	7·1
G_{23} (GPa)	–	–	2·5
Density ρ (kg/m^3):	–	7600	1600
d_{31} (pm/V)	23·0	−166	–
d_{32} (pm/V)	4·6	−166	–

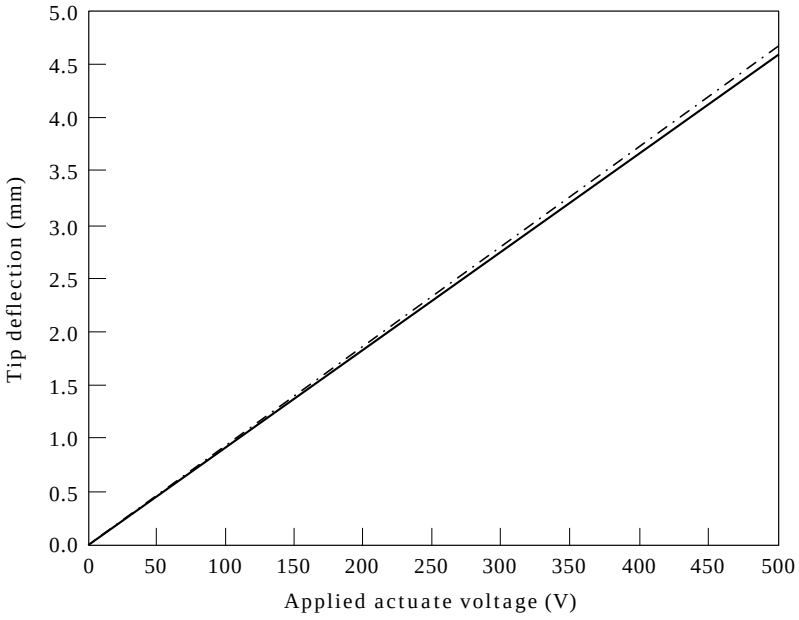

Figure 3. Effect of actuate voltages on tip deflection of the KYNAR beam. ——, Present model; – · –, Koconis *et al*. [4].

5.2. SHAPE AND VIBRATION CONTROL OF LAMINATED PLATES

Having validated the model and finite element method code, we present a numerical example to demonstrate the use of this code for simulating the response of laminated composite plates with integrated piezoelectric sensors and actuators in active deformation and vibration control.

Figure 4 shows a laminated composite plate with integrated piezoelectric sensors and actuators as well as a closed control loop. The plate dimensions considered are $a = b = 400$ mm and $h = 0{\cdot}8$ mm. The plate is constructed of four layers of T300/976 unidirectional graphite/epoxy composites. PZT G1195N piezoceramics,

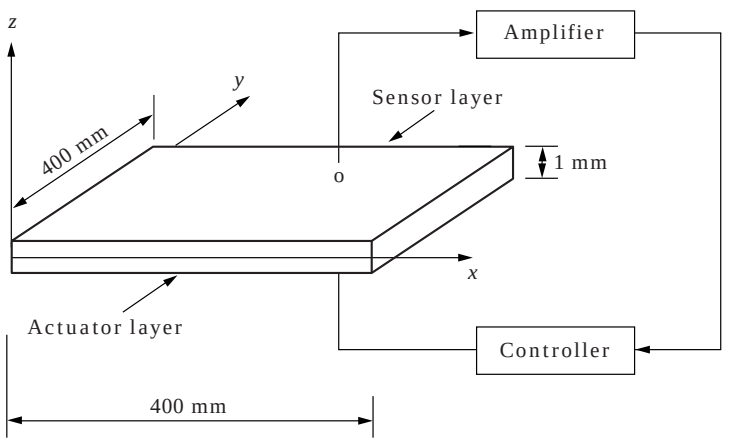

Figure 4. Laminated composite plate with integrated piezoelectric sensors and actuators.

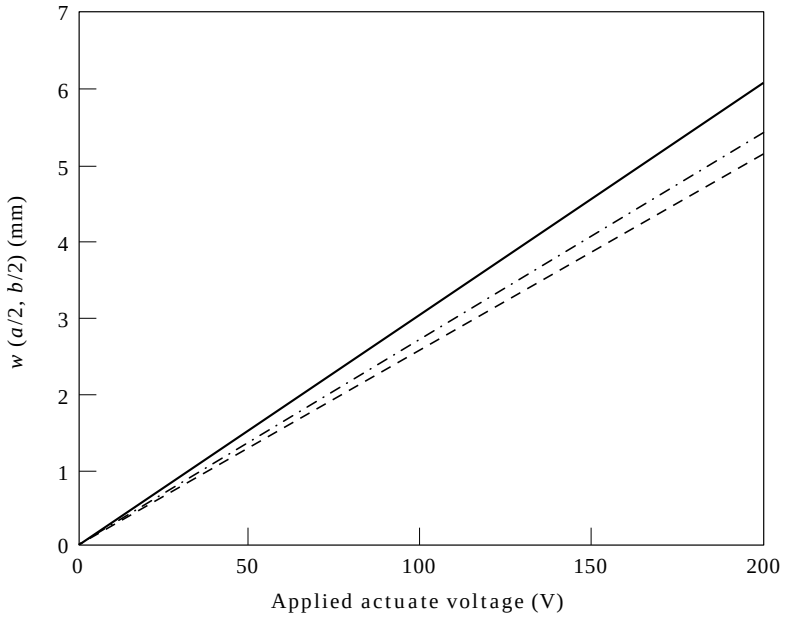

Figure 5. Effect of symmetric ply orientation on the transverse deflection. ——, [−15/15/15/−15]; – · –, [−30/30/30/−30]; – – –, [−45/45/45/−45].

which have a thickness of 0·1 mm, are symmetrically bonded on the upper and lower surfaces of the plate. The piezoceramics are modeled as two additional layers. The material properties of the T300/976 composities and PZT G1195N piezoceramics are shown in Table 1. Unless otherwise specified, [−30/30/30/−30]

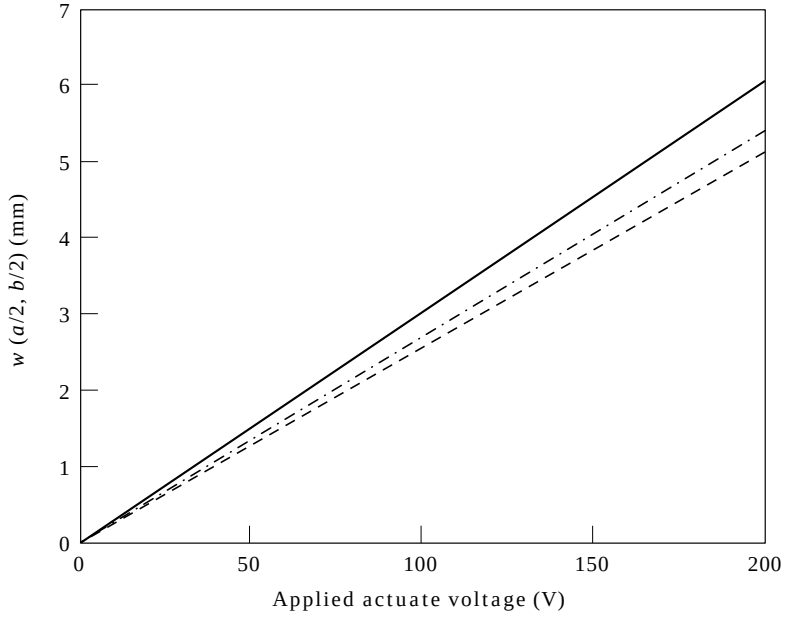

Figure 6. Effect of asymmetric ply orientation on the transverse deflection. ——, [−15/15/−15/15]; – · –, [−30/30/−30/30]; – – –, [−45/45/−45/45].

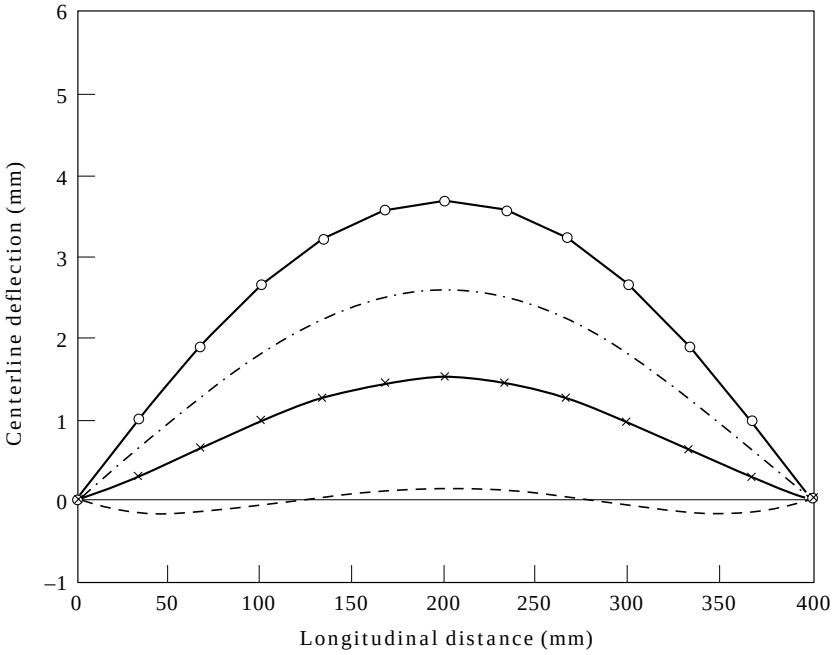

Figure 7. Centerline deflection of the plate under uniformly distributed load and different actuate voltages. ○, 0 V; – · –, 40 V; ×, 80 V; – – – 130 V.

symmetric angle-ply laminate layup is used. The plate is discretized into identical 8×8 plate elements. The simple supported boundary condition is considered:

$$v_0 = w_0 = \frac{\partial w_0}{\partial y} = 0 \qquad \text{at} \quad x = 0, a$$

$$u_0 = w_0 = \frac{\partial w_0}{\partial x} = 0 \qquad \text{at} \quad y = 0, b.$$

First, the static analysis and deformation control of the composite plate are presented. In the static analysis, all the piezoceramics on the upper and lower surfaces of the plate are used as actuators. The upper layer is polarized in the direction of the applied voltages and the lower layer is polarized in the opposite direction of the applied voltages. Equal-amplitude voltages with an opposite sign are applied across the thickness of the upper and lower piezoelectric layers respectively.

Figure 5 shows the variational tip deflection (centre point deflection) for different applied actuate voltages under different symmetric angle-ply orientation. It is observed that with an increase of the angle, a decrease of tip deflection under certain applied actuate voltage is observed. Figure 6 shows the effect of antisymmetric angle-ply orientation on the tip deflection of the laminated plate. Similarly, the increase of the angle for the antisymmetric angle-ply layup has an inverse influence on the plate's transverse deflection.

The effect of the actuate voltages on the shape control of the plate is also investigated. The plate is originally flat and then is exposed to a uniformly

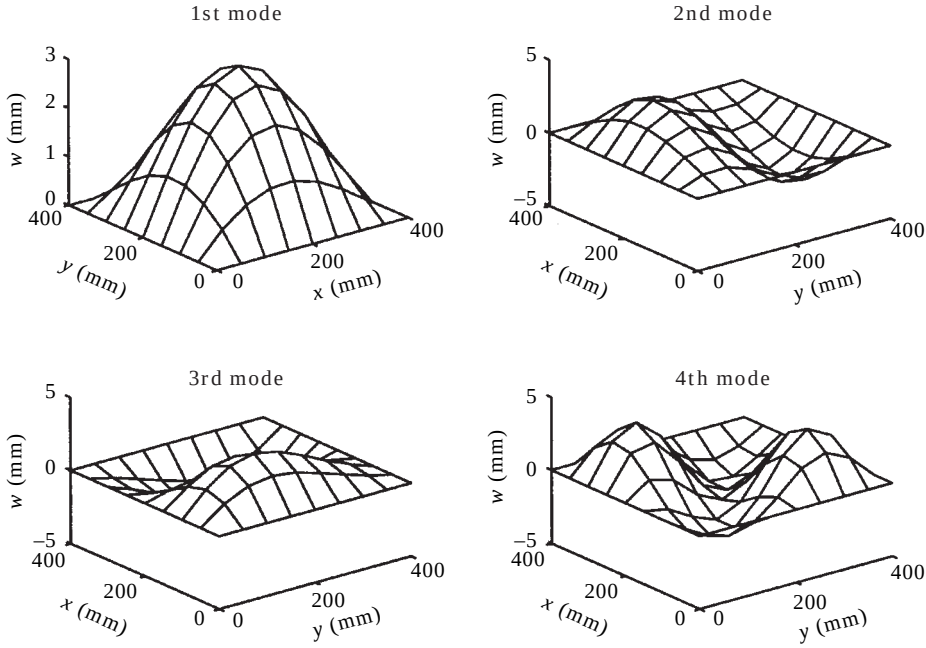

Figure 8. The first four vibration modes of the plate.

distributed load of $50\,N/m^2$. To flatten the plate, active voltage is input incrementally in the numerical simulation and the calculations proceeded with until the centerline deflection of the plate is reduced to a desired tolerance. Figure 7 shows the calculated centerline deflection of the composite plate under different actuate voltages. It can be concluded from Figure 7 that with proper piezoelectric actuators and actuate voltage, it is feasible to generate enough forces to control the shape of laminated composite plates.

The same configuration of the laminated composite plate given in Figure 4 is considered again to carry out the simulation of active free vibration suppression of the composite plate using the integrated sensors and actuators. In active vibration suppression, the upper piezoceramics are served as sensors and the lower

TABLE 2

Calculated natural frequencies of the plate (rad/s)

	Laminate ply orientation					
Natural frequency	$[-15/15]_s$	$[-30/30]_s$	$[-45/45]_s$	$[-15/15]_{as}$	$[-30/30]_{as}$	$[-45/45]_{as}$
1	165·573	174·007	178·191	165·611	174·748	179·437
2	354·818	383·470	401·851	355·432	388·594	424·174
3	481·046	464·894	452·816	473·784	452·083	424·174
4	637·596	658·804	670·703	644·601	679·143	697·131
5	688·555	754·180	826·348	681·514	739·077	821·397
6	935·439	936·055	858·164	943·816	914·986	824·449

$[\cdot/\cdot]_s$ = symmetric, $[\cdot/\cdot]_{as}$ = antisymmetric.

ones as actuators. The piezoceramics are evenly divided into four sensors and actuators. So, each sensor and actuator is meshed with 16 identical elements.

Table 2 shows the first six natural frequencies of the composite plate under different symmetric and antisymmetric angle-ply laminate layup and Figure 8 shows the first four vibration modes of the plate. It can be seen from Table 2 that for both symmetric and antisymmetric angle-ply orientation, the increase of the angle results in the increase of the first two natural frequencies. Under the same orientation angle, the symmetric angle-ply laminated plates have smaller first two natural frequencies compared with those of antisymmetric layup.

To control the free vibration of the plate, the collocated sensors and actuators should be coupled into sensor/actuator (S/A) pairs through closed control loops. In the present work, a simple negative velocity feedback control algorithm is used. It is assumed that the composite plate is vibrating freely due to an initial disturbance. The modal superposition technique is used to decrease the size of the problem. The first six modes are used in the modal space analysis and an initial modal damping ratio for each of the modes is assumed to be 0·8%. The Newmark-β direct integration method is then used to calculate the transient response of the plate. The parameters γ and β are taken as 0·5 and 0·25 respectively.

Figure 9 shows the effect of feedback control gain G on the transient response of the plate. It can be seen that with higher control gain, the vibration of the plate

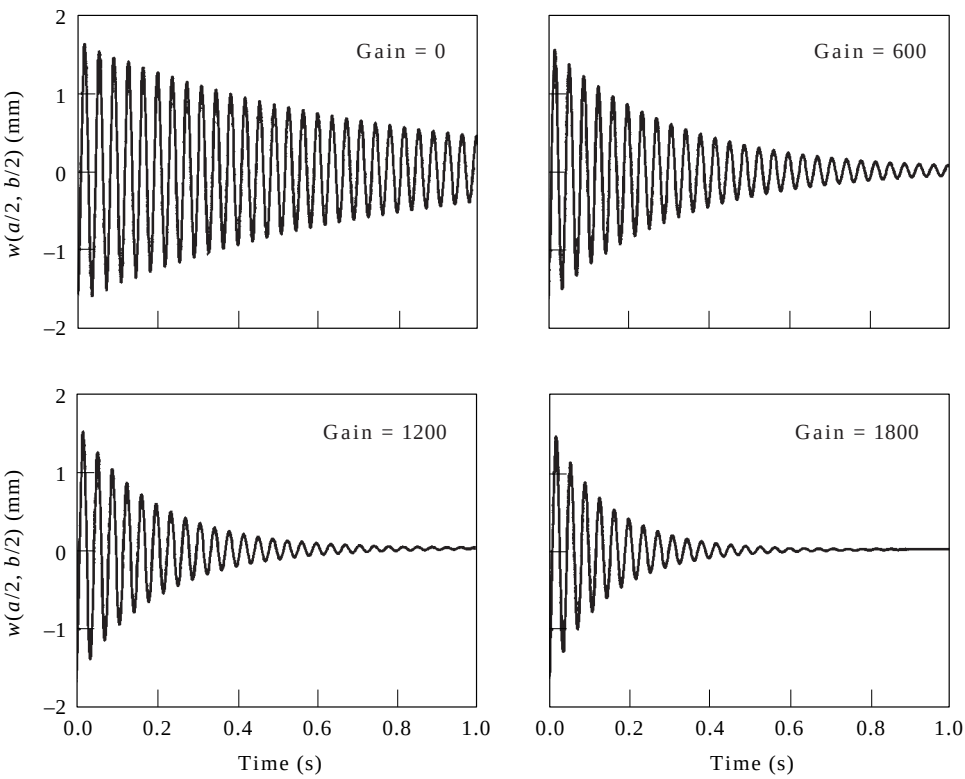

Figure 9. The effect of feedback control gain G on the plate's response.

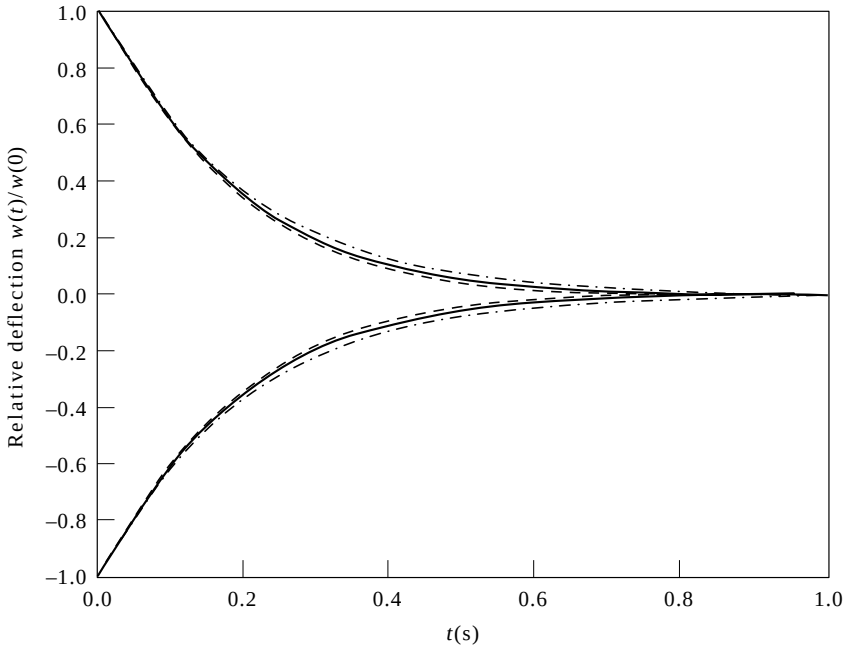

Figure 10. Effect of symmetric ply orientation on the plate's response ($G = 1200$). – – –, $[-15/15/15/-15]$; —, $[-30/30/30/-30]$; – · –, $[-45/45/45/-45]$.

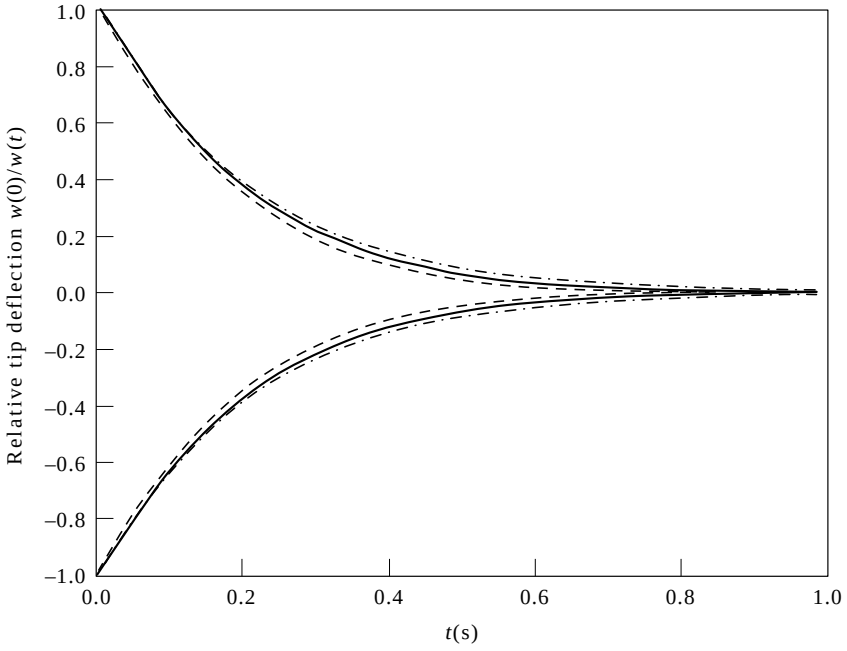

Figure 11. Effect of asymmetric ply orientation on the plate's response ($G = 1200$). – – –, $[-15/15/-15/15]$; —, $[-30/30/-30/30]$; – · –, $[-45/45/-45/45]$.

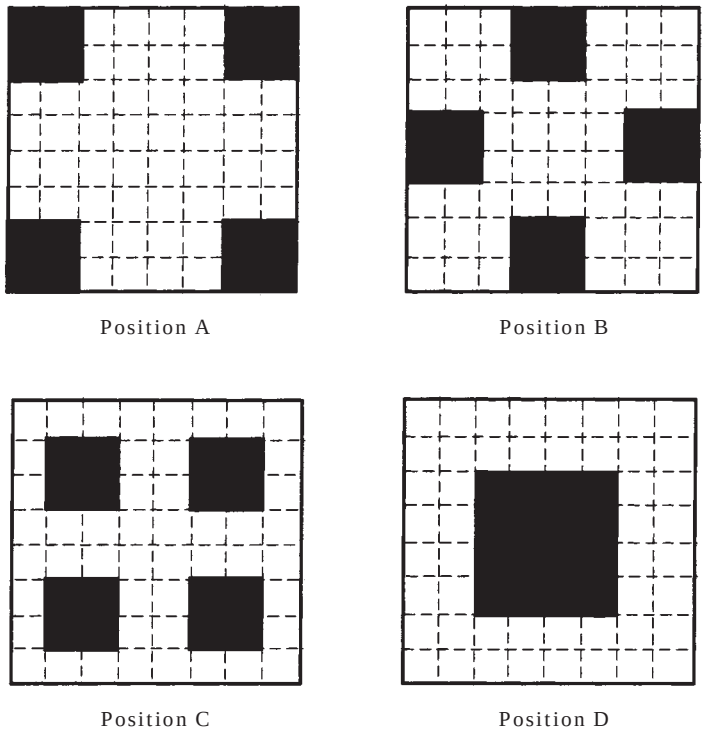

Figure 12. The position of sensor/actuator pairs.

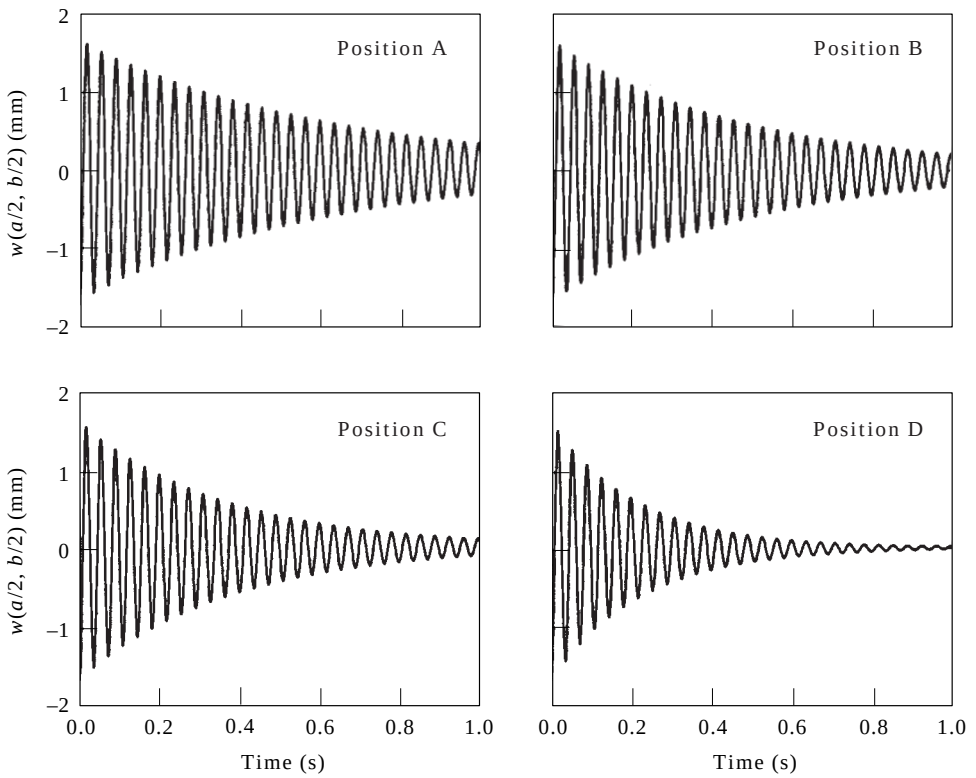

Figure 13. The effect of sensor/actuators' position on the plate's response ($G = 5000$).

Figure 9 shows the effect of feedback control gain G on the transient response of the plate. It can be seen that with higher control gain, the vibration of the plate is damped out more quickly. Figures 10 and 11 show the ply orientation on the plate's response. It is clear that the increase of the angle has an inverse effect on the vibration control of the plate for both symmetric and antisymmetric angle-ply layup. However, this effect is negligible.

Finally, the effect of the sensor/actuator pair's position on the response of the simply supported plate is investigated. Four pairs of piezoelectric sensors/actuators are bonded on different positions of the upper and lower surfaces of the plate, as shown in Figure 12. Each sensor/actuator patch has dimensions of 100 mm $\times$ 100 mm. It can be seen from Figure 13 that when the sensor/actuator pairs are bonded on the center or the plate, the control effect is the best.

6. CONCLUSIONS

Based on the classical laminated plate theory, a finite element model is developed to study the shape control and active vibration suppression of laminated composite plates with integrated piezoelectric sensors and actuators. The formulations are derived using Hamilton's principle. By incorporating a simple negative velocity control algorithm, the sensors and actuators are coupled into piezo-pairs through a closed loop to provide active feedback control effect on the plates. The model is validated by comparing with existing results documented in the literature. Some numerical results are presented. The influence of stacking sequence and position of sensors/actuators on the response of the composite plate is evaluated. Using the model presented here, more complicated loading conditions and geometries can be analyzed. With some modification, the model can be easily extended to shell problems.

REFERENCES

1. W. S. Hwang and H. C. Park 1993 *AIAA Journal* **31**, 930–937. Finite element modeling of piezoelectric sensors and actuators.
2. A. Suleman and V. B. Venkayya 1995 *Journal of Intelligent Material Systems and Structures* **6**, 776–782. A simple finite element formulation for a laminated composite plate with piezoelectric layers.
3. K. Y. Lam, X. Q. Peng, G. R. Liu and J. N. Reddy 1997 *Smart Materials and Structures* **6**, 583–591. A finite element model for piezoelectric composite laminates.
4. D. B. Koconis, L. P. Kollar and G. S. Springer 1994 *Journal of Composite Materials* **28**, 415–458. Shape control of composite plates and shells with embedded actuators. I. Voltages specified.
5. K. Chandrashekhara and R. Tenneti 1995 *Smart Materials and Structures* **4**, 281–290. Thermally induced vibration suppression of laminated plates with piezoelectric sensors and actuators.
6. S. E. Miller and H. Abramovich 1995 *Journal of Intelligent Material Systems and Structures* **6**, 624–638. A self-sensing piezolaminated actuator model for shells using a first order shear deformation theory.
7. C. Q. Chen, X. M. Wang and Y. P. Shen 1996 *Computers & Structures* **60**, 505–512. Finite element approach of vibration control using self-sensing piezoelectric actuators.

8. X. Q. Peng, K. Y. Lam and G. R. Liu 1998 *Journal of Sound and Vibration* **209**, 635–650. Active vibration control of composite beams with piezoelectrics: a finite element model with third order theory.
9. P. Donthireddy and K. Chandrashekhara 1996 *Composite Structures* **35**, 237–244. Modeling and shape control of composite beams with embedded piezoelectric actuators.
10. P. Heyliger, K. C. Pei and D. Saravanos 1996 *AIAA Journal* **34**, 2353–2361. Layerwise mechanics and finite element model for laminated piezoelectric shells.
11. D. A. Saravanos, P. R. Heyliger and D. A. Hopkins 1997 *International Journal of Solids and Structures* **34**, 359–378. Layerwise mechanics and finite element for the dynamics anlaysis of piezoelectric composite plates.
12. S. K. Ha, C. Keilers and F. K. Chang 1992 *AIAA Journal* **30**, 772–780. Finite element analysis of composite structures containing distributed piezoeceramic sensors and actuators.
13. H. S. Tzou and C. I. Tseng 1990 *Journal of Sound and Vibration* **138**, 17–34. Distributed piezoelectric sensor/actuator design for dynamic measurement/control of distributed parameter system: a piezoelectric finite element approach.
14. H. S. Tzou and J. P. Zhong 1996 *Shock and Vibration* **3**, 269–278. Spatially filtered vibration control of cylindrical shells.
15. H. S. Tzou and R. Ye 1996 *Mechanical Systems and Signal Processing* **10**, 459–469. Pyroelectric and thermal strain effects of piezoelectric (PVDF and PZT) devices.
16. S. Kapuria, S. Sengupta and P. C. Dumri 1997 *Computer Methods in Applied Mechanics and Engineering* **140**, 139–155. Three-dimensional solution for simply-supported piezoelectric cylindrical shell for axisymmetric load.
17. J. Kim, V. V. Varadan, V. K. Varadan and X. Q. Bao 1996 *Smart Materials and Structures* **5**, 165–170. Finite-element modeling of a smart cantilever plate and comparison with expriments.
18. J. N. Reddy 1997 *Mechanics of Laminated Plates*: *Theory and Analysis*. Boca Raton: CRC Press.
19. C. K. Lee 1992 *Intelligent Structural Systems*. Amsterdam: Kluwer Academic, 75–167. Piezoelectric laminates: theory and experiment for distributed sensors and actuators.